Hadron production in Au+Au collisions from STAR fixed-target experiment

Hongcan Li[1,2,*] for the STAR Collaboration

[1]Key Laboratory of Quark and Lepton Physics (MOE) and Institute of Particle Physics, Central China Normal University, Wuhan 430079, China

[2]School of Nuclear Science and Technology, University of Chinese Academy of Sciences, Beijing 101408, China

Abstract. Strange hadrons have been suggested as sensitive probes for the medium properties of the nuclear matter created in heavy-ion collisions. A dense baryon-rich medium is formed during collisions at center-of-mass energies of a few-GeV. Since strange hadrons are produced near or below the threshold, their phase space distribution and yield ratio may provide strong constraints on the equation of state (EoS) of high baryon density matter. In this contribution, recent results on strange hadron production in Au + Au collisions at $\sqrt{s_{\mathrm{NN}}}$ = 3.2, 3.5, 3.9, 4.5, 5.2 and 6.2 GeV from the STAR experiment in fixed-target mode are presented. The transverse momentum spectra (p_{T}), rapidity density distributions (dN/dy) of strange hadrons and their yield ratios will be presented as a function of centrality and collision energy. An enhancement of the the $\Lambda/\mathrm{K}^0_{\mathrm{S}}$ yield-ratio is observed above $\sqrt{s_{\mathrm{NN}}}$ = 3.9 GeV. We will also explore the evolution of their kinetic freeze-out temperature T_{Kin} and average radial expansion flow velocity $\langle\beta_{\mathrm{T}}\rangle$ extracted from the Blast-Wave model in the reported energy range. The physics implications will be studied by comparing to model calculations.

1 Introduction

Relativistic heavy-ion collisions provide an excellent opportunity to study the quark-gluon plasma (QGP). Searching for the critical point of quantum chromodynamics (QCD), studying properties of QGP and exploring the QCD phase diagram are major physics goals of the STAR experiment at the Relativistic Heavy-Ion Collider (RHIC) where the Beam Energy Scan (BES) program was developed. In the BES-II program, in fixed-target (FXT) mode, the collision energy per nucleon pair in Au+Au collision reaches down to $\sqrt{s_{\mathrm{NN}}}$ = 3 GeV, where the baryon chemical potential of the created nuclear matter reaches 750 MeV. The properties of the collision system at this high baryon density are expected to be different compared to a QGP where partonic interactions dominate.

Hadrons containing s and/or $\bar{s}$ quarks are called strange hadrons. There is no initial net-strangeness in the colliding nuclei so all final state strange hadrons are produced by the collision process, which make strange hadrons a very sensitive probe of the properties of produced fireball [1–4]. At STAR FXT energies ($\sqrt{s_{\mathrm{NN}}}$ = 3 - 13.7 GeV), strange hadrons are produced near or below the threshold energy and their yields may provide strong constraints on the equation-of-state (EoS)of the medium created in heavy-ion collisions, especially in the case of the excitation function of multi-strange (anti-)hyperons.

*e-mail: lihc@mails.ccnu.edu.cn

2 Experiment and data analysis

For the BES-II program, STAR installed the following upgrades: the inner Time Projection Chamber (iTPC) and the end-cap Time of Flight (eTOF) [5, 6]. This improved the detector acceptance and particle identification capabilities. STAR then collected approximately 10 times more collision events than in BES-I, which provided more accurate measurements.

In these analyses, we used the dataset of Au+Au collisions at $\sqrt{s_{\rm NN}}$ = 3.2, 3.5, 3.9, 4.5, 5.2 and 6.2 GeV. TPC and TOF detectors are used for particle identification and for short-lived particle reconstruction. The strange hadrons $\rm K^0_S$, Λ and Ξ^- are reconstructed by using the hadronic decay channels: $\rm K^0_S \to \pi^+ + \pi^-$, $\Lambda \to p + \pi^-$ and $\Xi^- \to \Lambda + \pi^-$. The KFParticle Finder package was used for the strange hadron reconstruction process [7].

3 Results and discussion

3.1 Transverse momentum spectra and rapidity density distributions

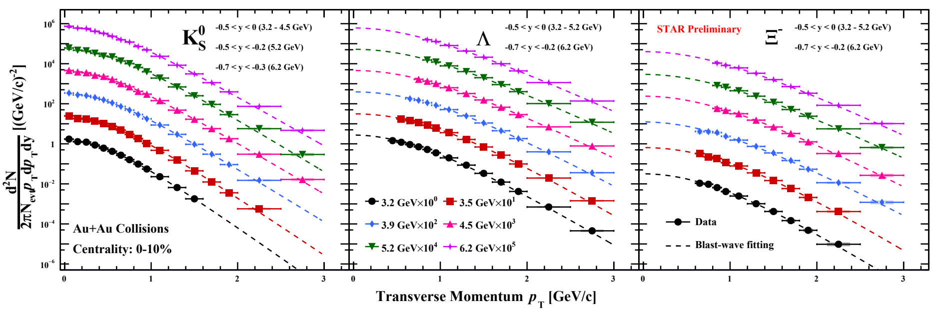

Figure 1. Transverse momentum spectra of $\rm K^0_S$, Λ and Ξ^- in central (0-10%) Au+Au collision at $\sqrt{s_{\rm NN}}$ = 3.2, 3.5, 3.9, 4.5, 5.2 and 6.2 GeV. The solid symbols are the measured data points. Dash lines correspond to Blast-Wave function fits.

Figure 1 shows the transverse momentum ($p_{\rm T}$) spectra of $\rm K^0_S$, Λ and Ξ^- in central (0-10%) Au+Au collisions. Because the measured $p_{\rm T}$ range cannot reach down to 0, we use Blast-Wave functions for fitting and extrapolating the data to unmeasured regions.

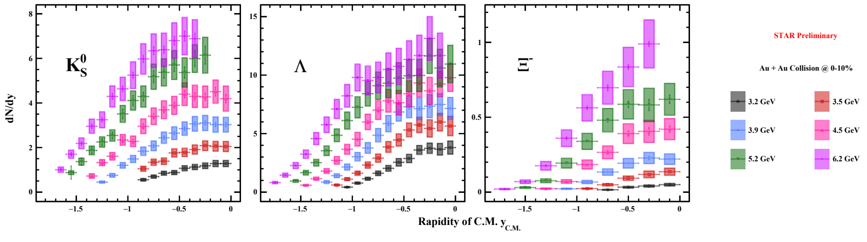

Figure 2. Rapidity distribution of $\rm K^0_S$, Λ and Ξ^- in central (0-10%) Au+Au collision at $\sqrt{s_{\rm NN}}$ = 3.2, 3.5, 3.9, 4.5, 5.2 and 6.2 GeV. The vertical lines are the statistical uncertainties, and the boxes are the systematic uncertainties.

Figure 2 shows the rapidity distributions (dN/dy) of $\rm K^0_S$, Λ and Ξ^- in central (0-10%) Au+Au collisions. They are obtained by integrating the $p_{\rm T}$ spectra using the measured data points where available and the extrapolation function for the unmeasured regions. Thanks to the large acceptance of the STAR detector and FXT mode setup, we can measure almost the full rapidity range from beam backward rapidity to mid-rapidity.

3.2 Baryon to meson ratio

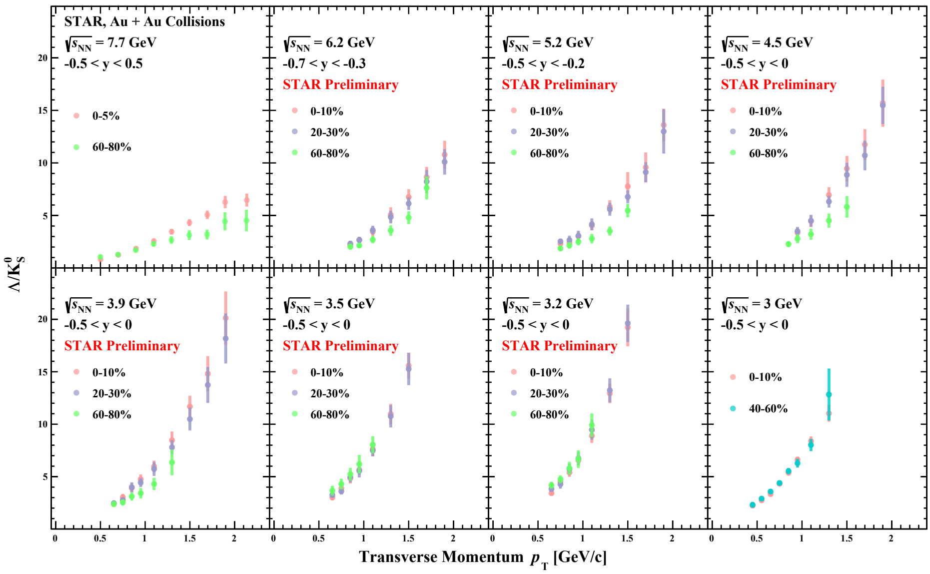

Figure 3. Λ/K^0_S ratio as a function of p_T in Au+Au collisions different centralities at $\sqrt{s_{NN}}$ = 3, 3.2, 3.5, 3.9, 4.5, 5.2, 6.2 and 7.7 GeV [8–10].

The baryon-to-meson ratio is regarded as a possible probe for a QGP formation. Figure 3 shows the Λ/K^0_S ratio as a function of p_T in different centralities. An enhancement of the Λ/K^0_S enhancement in central collisions with respect to peripheral collisions can be observed at $p_T > 1$ GeV, when the collision energy is above 3.9 GeV.

3.3 Kinetic freeze-out parameters

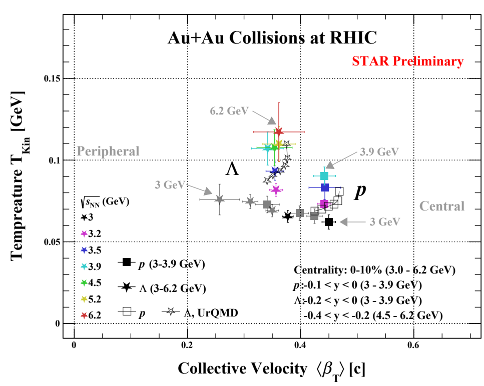

Figure 4. Kinetic freeze-out parameters $T_{Kin.}$ vs $\langle \beta_T \rangle$ in Au+Au Collisions at $\sqrt{s_{NN}}$ = 3, 3.2, 3.5, 3.9, 4.5, 5.2 and 6.2 GeV. The solid black and gray points represent results at 3 GeV with centrality of 0-10%, 10-20%, 20-40%, and 40-60% [8, 11]. The colored solid points represent results with centrality 0-10% at center-of-mass energies from 3.2 to 6.2 GeV. The hollow points represent UrQMD simulation results.

Figure 4 shows the kinetic freeze-out parameters temperature T_{Kin} and average radial expansion flow velocity $\langle\beta_{\mathrm{T}}\rangle$, which are obtained by fits with Blast-Wave functions to the p and Λ p_{T} spectra. As the collision energy increases from 3 to 6.2 GeV, T_{Kin} gradually rises. In addition, different freeze-out parameters $\langle\beta_{\mathrm{T}}\rangle$ and T_{Kin} are observed for p and Λ. The STAR results are qualitatively described by the transport model UrQMD.

4 Summary

In these proceeding, we report yield measurements of $\mathrm{K}^0_{\mathrm{S}}$, Λ and Ξ^- in Au+Au collisions at $\sqrt{s_{\mathrm{NN}}}$ = 3.2, 3.5, 3.9, 4.5, 5.2 and 6.2 GeV. Their p_{T} spectra and dN/dy are presented. An enhancement the $\Lambda/\mathrm{K}^0_{\mathrm{S}}$ enhancement is observed at $p_{\mathrm{T}} > 1$ GeV for energies above $\sqrt{s_{\mathrm{NN}}}$ = 3.9 GeV. Different values for $\langle\beta_{\mathrm{T}}\rangle$ are extracted for p and L at STAR-FXT energies.

Acknowledgement. This work was supported in part by the National Natural Science Foundation of China under Grant No. 12375134 and No.12305146, the National Key Research and Development Program of China (Grant No. 2024YFE0110103 and 2024YFA1611003), the Fundamental Research Funds for the Central Universities (Grant No. CCNU25JCPT017), and the Project for Young Scientists in Basic Research (No.YSBR-088) of the Chinese Academy of Science.

References

[1] P. Koch, et al. Physics Reports **142**, 167 (1986) 4. https://www.sciencedirect.com/science/article/abs/pii/0370157386900967
[2] C. Blume and C. Markert. Progress in Particle and Nuclear Physics **66**, 834 (2011) 4. https://www.sciencedirect.com/science/article/pii/S0146641011000834
[3] J.H. Chen, et al. Nuclear Science and Techniques **35**, 214, (2024) 12. http://www.nst.sinap.ac.cn/article/doi/10.1007/s41365-024-01591-2
[4] F. Liu, et al. SCIENTIA SINICA Physica, Mechanica & Astronomica **53**, 290003 (2023) 9. https://www.sciengine.com/SSPMA/doi/10.1360/SSPMA-2023-0167
[5] STAR Collaboration. Journal of Physics: Conference Series **779**, 012082 (2017) 1. https://iopscience.iop.org/article/10.1088/1742-6596/779/1/012082
[6] STAR Collaboration, CBM Collaboration eTOF Group. arXiv:1609.05102 **[nucl-ex]**. https://arxiv.org/abs/1609.05102
[7] I. Kisel. Journal of Physics: Conference Series **1602**, 012006 (2020) 1. https://dx.doi.org/10.1088/1742-6596/1602/1/012006
[8] STAR Collaboration. Journal of High Energy Physics **2024**, 139 (2024). https://link.springer.com/article/10.1007/JHEP10(2024)139
[9] STAR Collaboration. Physics Letters B **831**, 137152 (2022). https://www.sciencedirect.com/science/article/pii/S0370269322002866
[10] STAR Collaboration. Physics Review C **102**, 034909 (2020). https://journals.aps.org/prc/abstract/10.1103/PhysRevC.102.034909
[11] STAR Collaboration. Physics Review C **110**, 504911 (2020) 5. https://journals.aps.org/prc/abstract/10.1103/PhysRevC.110.054911